Tailoring assembly of reduced graphene oxide nano-sheets to control gas barrier properties of natural rubber nanocomposites

Giuseppe Scherillo [a], Marino Lavorgna [b], Giovanna G. Buonocore [b], Yanhu H. Zhan [c], Hesheng S. Xia [c*], Giuseppe Mensitieri [a*], Luigi Ambrosio [b]*

[a] Department of Chemical Engineering, of Materials and Industrial Production, University Federico II, P.leTecchio 1-80125 Napoli, Italy

[b] Institute of Composite and Biomedical Materials, National Research Council, P.le Fermi 1-80055 Portici (NA), Italy

[c] State Key Laboratory of Polymer Materials Engineering, Polymer Research Institute, Sichuan University, Chengdu, China

* *Corresponding authors: Marino Lavorgna (mlavorgn@unina.it), Hesheng Xia (xiahs@scu.edu.cn) and Giuseppe Mensitieri (mensitie@unina.it)*

CHEMICALS AND SAMPLE PREPARATION

The natural rubber latex (60 wt% of solid content in aqueous ammonium) with size distribution in the range from 0.015 to 3 μm, average diameter equal to 0.5 μm, was provided by Chengdu Fangzheng Co., Ltd (China). The number-average molecular weight of natural rubber is 300000. Flake Graphite (~75 μm) was obtained from Qingdao Tianhe Graphite Co., Ltd (China). Potassium permanganate ($KMnO_4$) and Hydrazine hydrate were obtained respectively from Chongqing Boyi Chemical Reagent Co., Ltd (China) and Chengdu Kelong Chemical Reagent Company (China). Concentrated sulfuric acid (H2SO4), hydrochloric acid (HCl) and Hydrogen peroxide (30%) as well as other reagents including vulcanization agent sulfur, zinc oxide, accelerator N-cyclohexyl-2-benzothiazolesulfenamide (CBS) and 2-mercaptobenzothiazole (MBT), antioxidant (4010NA), and stearic acid are all commercially available.

Reduced graphene oxide (RGO) platelets were obtained by oxidation of natural graphite flake according to the Hummer and Offeman method [1] and subsequent chemical reduction according to the method described by some of the authors in [2]. In details 16.7gr of NR latex was dispersed in different amounts of a 3.125mg/mL graphene oxide GO aqueous solution. Afterwards the GO platelets were in-situ reduced by hydrazine (GO/hydrazine hydrate ratio is 1.25:5 (g/mL)) under ultrasonic irradiation. In this stage the RGO platelets self-assembled to form a thick graphene layer on the surface of the latex particles (see Figure S1). The vulcanization additives, consisting of crosslinking sulfur (2.8 phr with respect to rubber), zinc oxide (5phr), stearic acid (3phr), antioxidant 4010NA (3phr), CBS accelerator (1.4phr) and mercaptobenzothiazolo accelerator (0.1phr), were added into the RGO/NR latex suspension and then the resulting dispersion was coagulated and filtrated. The obtained NR/RGO solid was ~~then~~ directly hot pressed under static pressure and *in-situ* vulcanized at 150°C. However, over the initial phase of vulcanization, i.e. scorch time, the NR/RGO solid was degassed to prevent the formation of micro- and macro-pores in the vulcanized samples. During this process, the solid polymer particles densely packed creating an excluded volume wherein RGO platelets form a segregated network structure. Conversely, when the NR/RGO solid was treated with a twin-roll mixing, the segregated network of latex particles was destroyed and the reduced graphene oxide platelets dispersed throughout the NR/RGO composites forming a well-dispersed not-segregated graphene structure. Composites with 0.94, 1.78, 3.38 and 5.15 %vol of RGO corresponding respectively at about 1.06, 2.0, 3.81, and 5.86 %wt of RGO, were prepared for both segregated and not-segregated morphology.

SUPPLEMENTARY TEM MICROGRAPHS

TEM analysis was performed by using a FEI TecnaiG2 F20 S-TWIN transmission electron microscope, operating at an accelerating voltage of 200 kV.

In order to observe the self-assembling of RGO nanoparticles on the surface of rubber latex particle, the NR latex containing RGO was adequately diluted and deposited on the stab for TEM analysis.
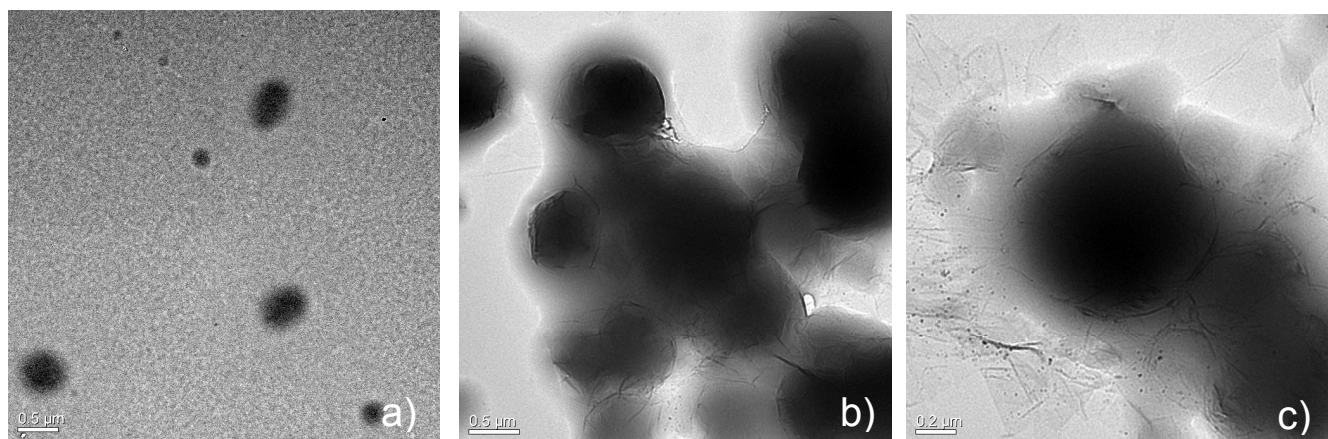

Figure S1. TEM images of a) diluted NR latex, b) and c) diluted NR latex with RGO nanoparticles.

The composites were cryomicrotomed by using a Leica EM UC6 equipment and ultra-thin sections thick about 70–80 nm were directly supported on a copper grid for observation. The cutting of the samples was performed to allow the determination of the average orientation of RGO platelets with respect to the surfaces of nanocomposite films.
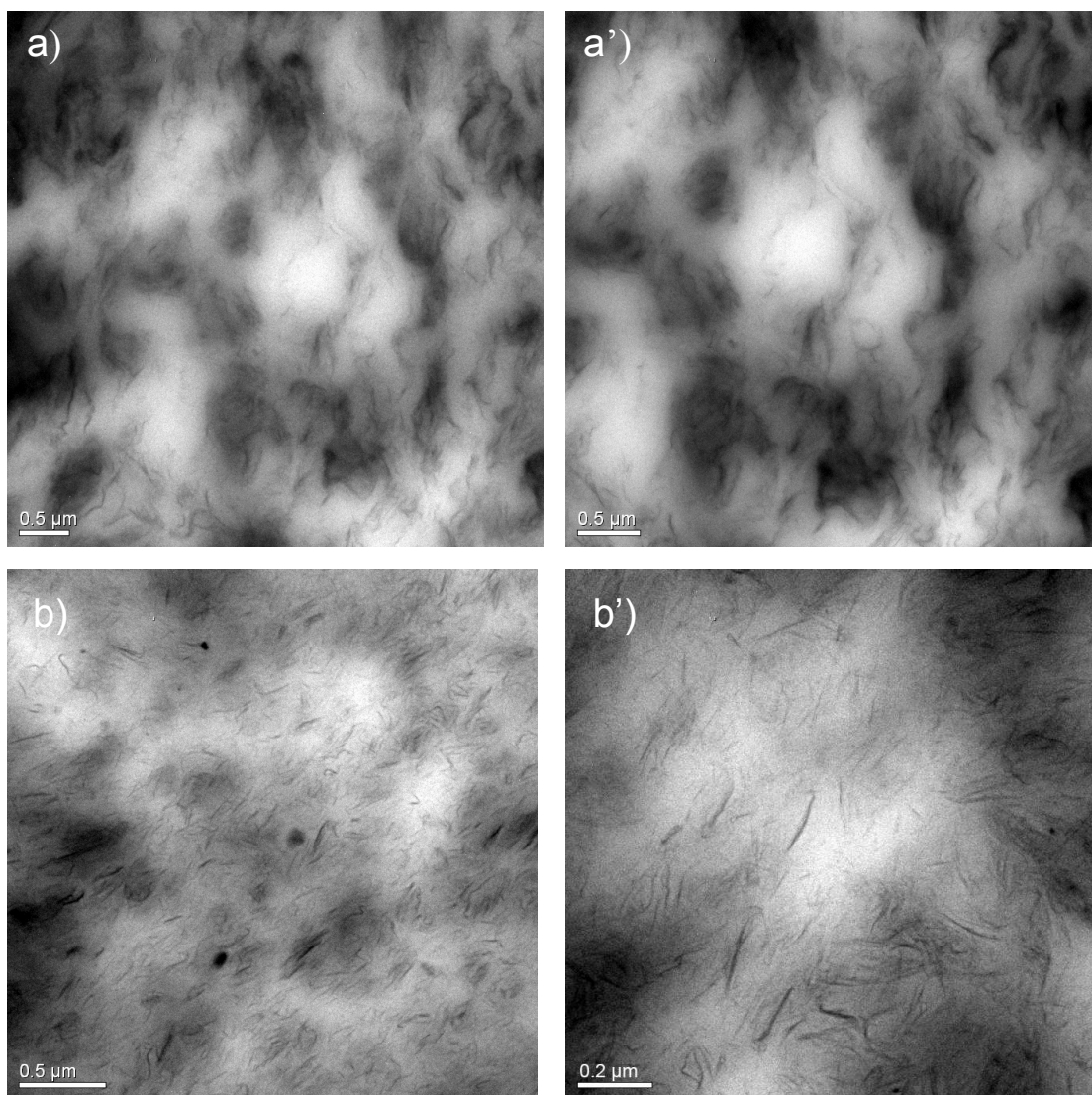
Figure S2. TEM images of NR/RGO composites with 5.15 vol% RGO prepared a) by self-assembly in latex and static hot pressing and b) by self-assembly in latex and twin-roll mixing. Figures a') and b') are magnified images of a) and b).
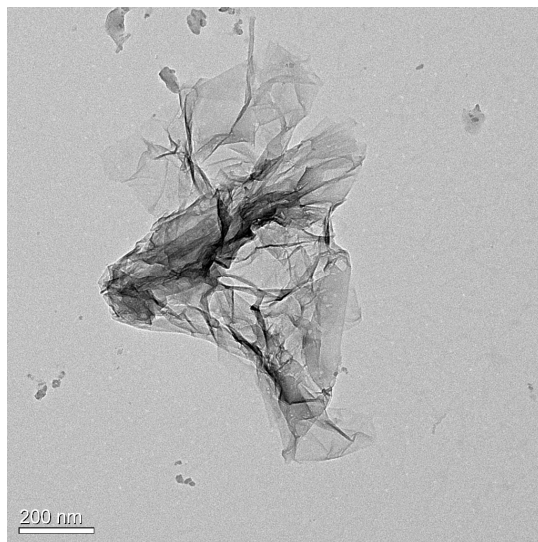
Figure S3. TEM image of single graphene platelet obtained according to the procedure described in the Section Chemicals and Sample Preparation.

PERMEATION MEASUREMENTS

Permeability tests were performed with pure gas in dry conditions, using a custom made permeabilimeter capable of working at several pressures and temperatures. A detailed description of the apparatus and of its working principle is reported in the literature [3]. The permeability value was evaluated on a nanocomposite sheet under a pressure difference of the gas of interest between the upstream side (at 1 atm) and the downstream side (under vacuum) of the sheet, by measuring the mass flux at steady state, J_{SS}, that is calculated from the rate of increase of downstream pressure. Permeability is defined as follows:

$$P = \frac{J_{SS}}{\Delta p / l} \qquad \text{Eq. S1)}$$

where l represents the thickness of polymer film and Δp is the gas pressure difference. In the present contribution, J_{SS} has been expressed in (cm^3 STP) cm^{-2} s^{-1} (where cm^3 STP represents the volume that the mass of gas permeated would occupy in standard temperature and pressure conditions), p has been expressed in atm and the film thickness in cm. In the case at hand the thickness is 0.0160 cm +/- 0.0003, while the area exposed to the gas flux was 4.52 cm^2. As a consequence permeability is expressed in $\frac{cm^3(STP) \cdot cm}{cm^3 \cdot s \cdot atm}$. Permeation experiments were performed at 30, 38 and 48°C for O_2, N_2 and CO_2.

EXPERIMENTAL RESULTS FOR PERMEABILITY AND RELATIVE PERMEABILITY

In Figure S4 a) and b) are reported respectively the permeability of the three gases investigated at 38°C for the not-segregated and the segregated morphology as a function of the volumetric fraction of RGO, $\phi_{graphene.}$. The results of permeation experiments indicate that, regardless the morphology, the permeability of the three gases are always in the following order: $P_{CO_2} \gg P_{O_2} \gg P_{N_2}$. The same trend is exhibited also at the other two investigated temperatures.
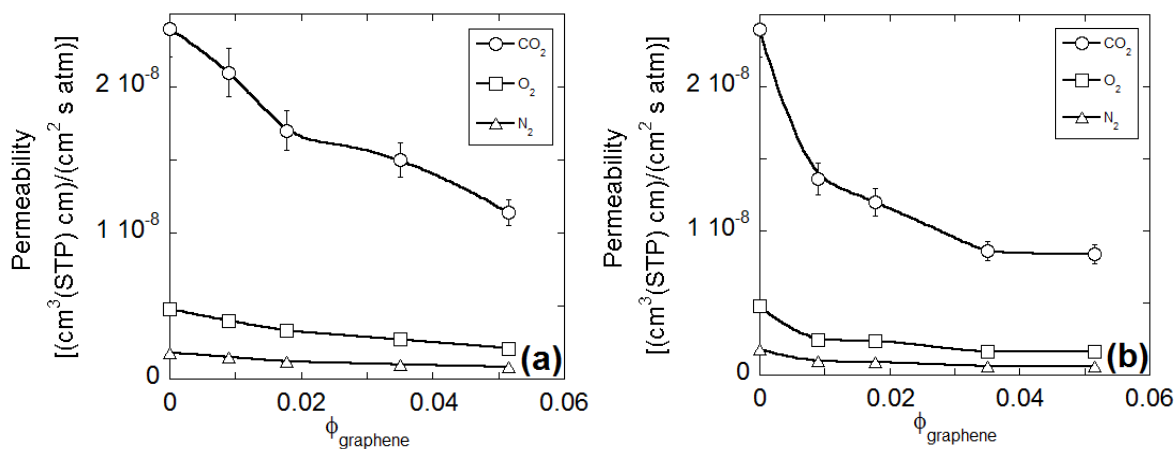
Figure S4. Permeability of the three gases investigated at 38°C for the samples with respectively not-segregated morphology (a) and segregated morphology (b) as a function of the volumetric fraction of RGO. The standard deviation is equal to 4% of the absolute average permeability value.
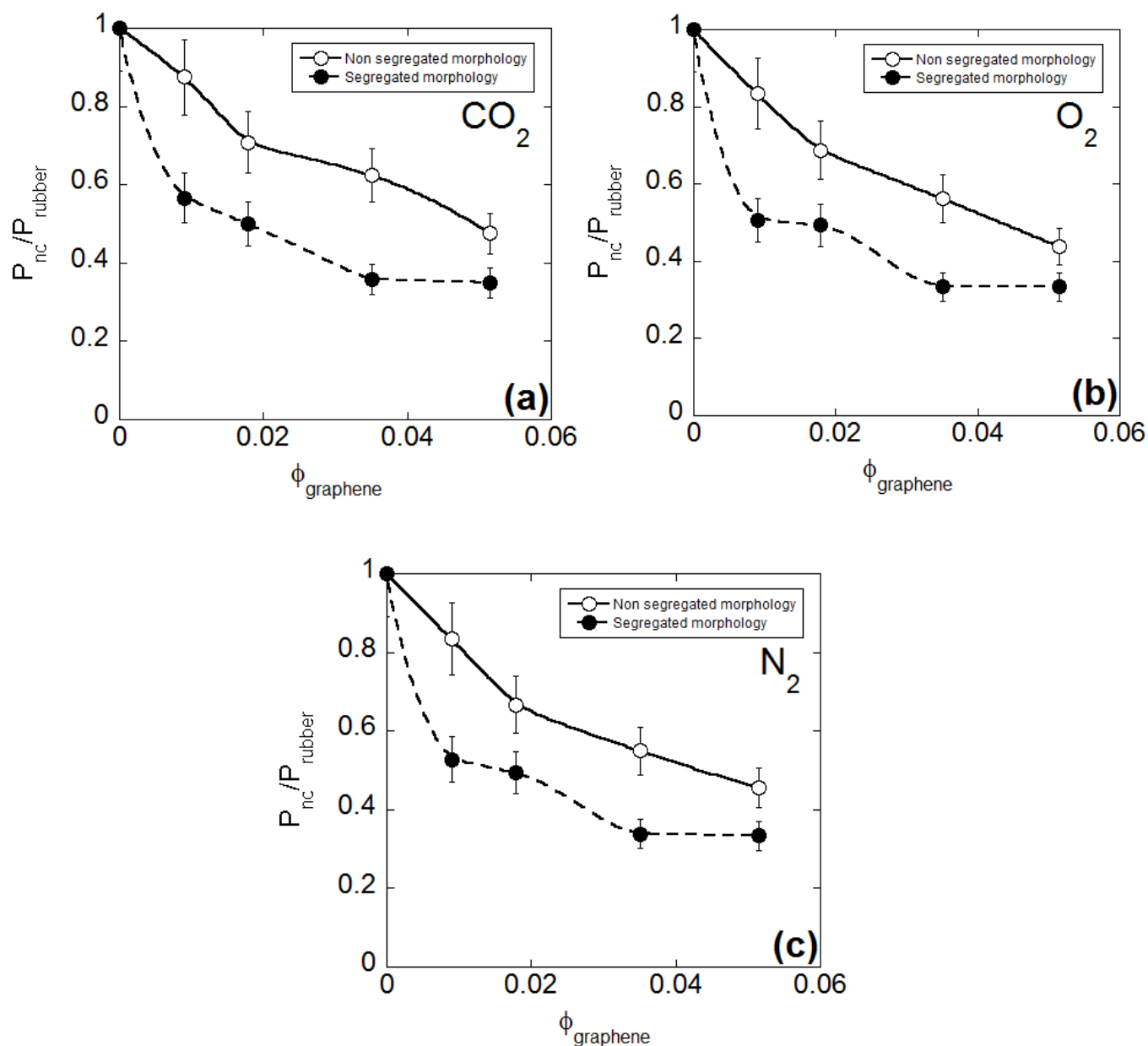
Figure S5. Comparison of the relative permeability at 38°C of a) CO_2, b) O_2 and c) N_2 for the samples with not-segregated and segregated morphology as a function of the volumetric fraction of RGO. The standard deviation is equal to 4% of the absolute average permeability value.

Gas permeabilities display a marked decrease, for both morphologies, as the volumetric fraction of RGO increases, although the shapes of the curves present some dissimilarities. A comparison of the features of the two investigated morphologies for each of the analysed gas, is reported in Figure S5 a), b) and c). In particular, it is reported the case at 38°C, but a qualitatively similar behaviour was also obtained at 30 and 48°C. The segregated morphology displays, at each volumetric fraction of

RGO, a significantly lower permeability for all the gases. Furthermore evidence of a double step decrease in the permeability curves emerges for all gases in the case of the segregated morphology. In particular, a marked decrease was observed in correspondence of the lowest RGO concentration investigated. Conversely, in the case of the not-segregated morphology, the permeability of the gases reported steadily decreases in the whole range of RGO concentration, with an initial slope that is markedly smaller than in the case of the segregated morphology. This peculiar difference between the two morphologies is likely related to the different arrangement of the RGO plate-like particles displayed by the two morphologies.

THEORETICAL MODELS: THE BHARADWAJ MODEL

The model provides the ratio of steady-state permeability of low molecular weight penetrant for the heterogeneous biphasic system to the steady-state permeability of the matrix material in the case of a composite in which the filler arrangement consists of impermeable disk plate-like particles, each of the same size and uniformly oriented or randomly oriented, with reference to the surface of the film. According to the model the following expression for the relative permeability holds:

$$P_c / P_m = \frac{1 - \phi}{1 + (L/2W)(2/3)\phi(s + 0.5)} \qquad \text{Eq. S2)}$$

where P_c and P_m represent, respectively, the effective permeability of the composite and that of the neat matrix, ϕ represents the volumetric fraction of the filler, and L/W represents the aspect ratio of the plate-like filler, L being the main dimension of the particles and W their thickness. Orientation of the particles is accounted for by introducing the parameter s that is defined as:

$$s = \frac{1}{2}\left\langle 3\cos^2 \theta - 1 \right\rangle \qquad \text{Eq. S3)}$$

where θ represents the angle between the normal to the film, $\underline{n}$, and the normal to the filler particle, $\underline{p}$ and in the case of random orientation of the particles it is equal to 0.

THEORETICAL MODELS: THE MOOSAVI MODEL

In a recent paper Moosavi et al [5] have introduced a model aimed at the prediction of the steady-state thermal conductivity of a composite material in which a homogeneous matrix,

displaying a constant thermal conductivity, is filled with an array of multicoated spherical inclusions in which each coating layer is characterized by a different constant thermal conductivity. Solving the linear Laplace equation describing the steady state energy balance over all the volume of the heterogeneous system, implicit numerical solutions based upon numerical series have been obtained. In particular, using a linear truncation procedure, explicit approximate solutions have been determined for three possible arrangements of the inclusions (i.e simple cubic (SC), body-centred cubic (BCC) and face-centred cubic (FCC)), all displaying the following form:

$$k_{eff} = 1 - 3F / \delta \qquad \text{Eq. S4)}$$

where k_{eff} represents the ratio of the equivalent conductivity of the composite to the conductivity of the matrix surrounding the multicoated spheres, F represents the multicoated sphere volumetric fraction and δ is a summation term which depends upon the order of truncation and on kind the spatial arrangement of the multicoated spheres. In the present contribution the order four solution (highest accuracy expression for approximate explicit solution derived in [5]) has been implemented, and in this case the summation term δ is given by:

$$\delta = -1/L_1^N + F + c_1 L_2^N F^{10/3} \frac{1 + c_4 L_3^N F^{11/3}}{1 - c_2 L_2^N F^{7/3}} + c_3 L_3^N F^{14/3} + c_5 L_4^N F^6 + c_6 L_5^N F^{22/3} + O(F^{25/3}) \quad \text{Eq. S5)}$$

where:

$$L_n^i = \frac{(2n-1)(k_{i-1,i} - 1) + \left[2n(k_{i-1,i} + 1) - 1\right]L_n^{i-1}(a_{i-2}/a_{i-1})^{4n-1}}{\left[(2n-1)(k_{i-1,i} + 1) + 1\right] + 2n(k_{i-1,i} - 1)L_n^{i-1}(a_{i-2}/a_{i-1})^{4n-1}} \qquad \text{Eq. S6)}$$

In Eq. S5) $O(F^{25/3})$ is a function which is an infinitesimal of order higher than $F^{25/3}$ when F tends to zero whereas N represents the number of phases of the system. In the multicoated framework one phase is formed by the core (the spheres with lowest radius), and the number of phases organized as multi-coating layers in a sphere is therefore equal to N-1, while the Nth phase is given by the matrix phase surrounding the multicoated spheres. Therefore a_i represents the radius of the sphere coated by layer $i+1$ for $i = 1,....,N$-1. In addition the notation $a_0 = 0$ is assumed. Finally $k_{i-1,i}$ represents the thermal conductivity ratio between the phase i-1 and phase i. Finally the six constant coefficients c_i depend on the kind of arrangement (i.e SC, BCC and FCC and reported in [5]).

It is now worth making some comments about the extension of this approach to the case of mass transport. The parallel between the model expression for the steady state energy transport and the steady state mass transport is readily made in the special case of simple ideal Fickian behaviour for

the constitutive expression of mass flux. In fact, the permeation of a low molecular weight compound in a polymer follows ideal Fickian behaviour, if: 1) the compound displays a constant solubility, S, within the polymer as a function of its pressure in the gaseous phase (liner sorption isotherm), and 2) the constitutive expression for penetrant mass flux is given by $J = -D_{12}\nabla C$, with the mutual diffusivity coefficient D_{12} of the penetrant (1) in the polymer (2) that is independent of penetrant concentration, C. In this case the following equation is obtained:

$$J = -D_{12} \cdot \nabla C = -D_{12} \cdot \nabla(Sp) = -D_{12} \cdot S \cdot \nabla p = -P \cdot \nabla p \qquad \text{Eq. S7)}$$

with $S = C/p$ where S is the penetrant solubility. Therefore Eq. S7) is formally equivalent to the constitutive expression for the conductive energy flux $J = -k\nabla T$ and consequently the steady-state mass balance and the steady-state thermal energy balance becomes formally equivalent, with P playing the role of k and p playing the role of T.

The assumptions 1) and 2) are reasonable in the case of mass transport of penetrants in rubbery polymer systems at low pressures, in the cases in which no specific interactions take place between the penetrant molecules and the polymer backbone and/or the filler and no significant swelling of the matrix is induced by the penetrant sorption. It is worth noting that the assumption that the penetrant permeability is not function of its concentration has been made also in the development of the models of Bharadwaj [4].

THEORETICAL MODELS: THE MODIFIED MOOSAVI MODEL

The behaviour of samples displaying the segregated morphology has been described using an *ad hoc* modified version of the multicoated model proposed by Moosavi et al [5]: in particular, it has been assumed that the heterogeneous sample is constituted by a rubber matrix embedding coated rubber spheres, the coating of the spheres being formed by RGO platelets. On the basis of TEM images, a simplified morphology has been assumed to construct the model as schematized in the sketches reported in Figure 2 of the letter. In particular, the relevant assumptions related to this simplified morphology are:

1) the system can be schematized as formed by pure permeable close-packed polymeric spheres of same size on which impermeable RGO platelets segregate.

2) these spheres, whose surface is partially or fully covered by RGO particles, are embedded in a matrix formed by the permeable pure polymer.

The RGO particles are assumed to be distributed along the surface of spheres arranged in discrete single layers of thickness d equal to 3nm and aspect ratio equal to 167. It is expected that increasing the concentration of RGO the permeability decreases since more and more surface of the spheres is covered by impermeable graphene particles. Introducing an average surface RGO concentration this effect can be treated assuming that the system under investigation is formed by equal size, one-layer coated, spheres embedded in the pure polymeric bulk matrix. To simplify mathematical treatment, each sphere is assumed as being made of an inner pure polymeric core covered by a continuous coating layer. This coating has a thickness equal to d displaying a permeability which is a decreasing function of the RGO concentration. In particular the permeability of this coating is taken as decreasing from a value equal to the one of the pure polymer to the zero value in correspondence of a threshold value of RGO concentration. This value corresponds to the minimum value of RGO concentration for which the polymeric spheres are totally covered by this impermeable layer and act as impermeable spheres embedded in a permeable matrix. This simplified homogenization approach allows to perform estimates of permeation behaviour, without the necessity of retrieving experimental information on RGO coverage statistics of rubber spheres, that is difficult to assess.

More in detail a coating threshold is first calculated by equating the area of the total surface of RGO particles, A_{totg}, to the total area of the surface of the rubber spheres, A_{tots} :

$$A_{tots} = \xi \cdot V_{tot} \cdot 3 / R = A_{totg} = \frac{\phi^{*}_{graphene} \cdot V_{tot}}{d} \qquad \text{Eq. S8)}$$

where R, V_{tot}, d, $\phi^{*}_{graphene}$ represent respectively the radius of the uncoated spheres, the total volume of the system, the thickness of each RGO plate-like particle and the critical RGO volumetric fraction which correspond to the coating threshold. Actually the radius of the uncoated and that of coated spheres can be safely assumed to be the same in views of the fact that $d/R \ll 1$. Finally, ξ represents the packing factor for the topology under consideration. We assume here that the spheres have a close packed ordered arrangement where all the spheres touch each other. Three possible structures are then possible: simple cubic (SC) for which $\xi = \pi/6$, body centred cubic (BCC) for which $\xi = (\pi/24) \cdot 3^{1.5}$ and face centred cubic (FCC) for which $\xi = (12) \cdot 2^{1.5}$.

Solving equation S8) for $\phi^{*}_{graphene}$ the following relationship is obtained:

$$\phi^{*}_{graphene} = 3 \cdot d \cdot \xi / R \qquad \text{Eq. S9)}$$

The permeability of the external shell of RGO coated rubber spheres to be used in the Moosavy model, P_{shell}, is lower than that of the rubber itself since RGO particles being impervious to low molecular weight penetrants, act as an obstacle to diffusion. The value of P_{shell} is then calculated by imposing that its value is equal to that of a pure rubber material reduced by a factor A_{free}/A_{tots} assuming that the permeability decrease results from the reduction of the total area of surface exposed to the mass flux, A_{tot}. Thus the *equivalent* penetrant permeability can be defined for the coating layer, P_{shell}, as:

$$P_{shell} = P_{rub}\frac{A_{free}}{A_{tot}}$$ Eq. S10)

where P_{rub} and A_{free}, represent respectively the penetrant permeability of the rubber material and the average area of the uncoated surface of a sphere. The higher is the amount of the RGO coating the lower is P_{shell}, that attains a value equal to zero for $\phi_{graphene} \geq \phi^*_{graphene}$. The value of A_{free} can be evaluated as:

$$A_{free} = A_{tots} - nA_s$$ Eq. S11)

with n and A_s representing, respectively, the total number of RGO particles and the area of the of plate-like particle exposed to mass flux. The following relationship holds for A_s:

$$nA_s = \frac{\phi_{graphene} \cdot V_{tot}}{d}$$ Eq. S12)

According to Eq. S10) and S11) and considering that only non negative values of A_{free} are meaningful, the following expression is obtained:

$$\left\{ \begin{array}{ll} P_{shell} = P_{rub}\left(\dfrac{\left(\dfrac{\xi \cdot V_{tot} \cdot 3}{R} - \dfrac{\phi_{graphene}V_{tot}}{d}\right)}{\dfrac{\xi \cdot V_{tot} \cdot 3}{R}}\right) = \left(\dfrac{\dfrac{\xi \cdot 3}{R} - \dfrac{\phi_{graphene}}{d}}{\dfrac{\xi \cdot 3}{R}}\right) & for \quad 0 \leq \phi_{graphene} \leq \phi^*_{graphene} \\ and & \\ P_{shell} = 0 & for \; \phi_{graphene} \geq \phi^*_{graphene} \end{array} \right.$$ Eq. S13)

The values of P_{shell} determined by Eq. S13) are then used in the Moosavi model, according to the extension of this model to the case of mass transport.

To summarize, the nanocomposite with a segregated morphology has been modelled as single coated rubber spheres with a radius, *R,* equal to 450 nm (average radius as determined by TEM analysis) embedded in a pure rubbery matrix. Each sphere is assumed to be coated by a shell with a thickness equal to *d* (i.e. about 3nm) whose permeability is provided by Eq. S13). It is worth noticing here that in the development of this approach, we have also assumed that as the volume fraction of RGO particles increases, first a shell is gradually formed by graphene particles. Only after a uniform shell of RGO particles is deposited on the rubber spheres, further increase of volume fraction of RGO promotes the formation of regions of coating with a thickness larger than *d*.

The results reported in this paper were obtained assuming a simple cubic arrangement of the spheres. It is worth mentioning that both the models discussed previously do not account for possible interactions between penetrant molecules and RGO filler but only for the geometrical effects related to the presence of impermeable particles. Although data do not collapse onto a single 'master' curve, as should be expected if only geometric effects come into play, this mismatch is estimated to be in the range of possible experimental error and consequently the effect of interactions have been neglected.

REFERENCES

(1) Hummers W.S.; Offeman, R.E. Preparation of Graphitic Oxide. *J. Am. Chem. Soc.* **1958**, 80, 1339-1339.

(2) Zhan, Y.; Wu, J.; Xia, H.; Yan, N.; Fei, G.; Yuan, G. Dispersion and Exfoliation of Graphene in Rubber by an Ultrasonically-Assisted Latex Mixing and In situ Reduction Process. *Macromol. Mater. Eng.* **2011**, 296, 590-602.

(3) Nicodemo, L.; Marcone, A.; Monetta, T.; Mensitieri, G., Bellucci, F. Transport of water dissolved-oxygen in polymers via electrochemical technique. *J. Membr. Sci.* **1992**, 70, 207-215.

(4) Bharadwaj, R.K. Modeling the barrier properties of polymer-layered silicate nanocomposites. *Macromolecules* **2001**, 34, 9189-9192.

(5) Moosavi, A.; Sarkomaa, P.; Polashenski, J.R.W. The effective conductivity of composite materials with cubic arrays of multi-coated spheres. *Appl. Phys. A: Mater. Sci. Process.* **2003**, A 77, 441-448.